Articles

Precisely Defined Amphiphilic Graft Copolymers

Erik B. Berda, Rachel E. Lande, and Kenneth B. Wagener*

The George and Josephine Butler Polymer Research Laboratory, Department of Chemistry, University of Florida, Gainesville, Florida 32611-7200

Received March 1, 2007; Revised Manuscript Received September 26, 2007

ABSTRACT: A family of precisely defined amphiphilic polyethylene-*g*-poly(ethylene glycol) copolymers has been synthesized using ADMET polycondensation chemistry. Altering the graft distribution and graft end group controls the morphology of the material: the polymers can be either semicrystalline or rendered completely amorphous. The precise monomer structures have been confirmed by ^{1}H and ^{13}C NMR, high-resolution mass spectrometry, and elemental analysis; the corresponding polymer structures have been confirmed by ^{1}H and ^{13}C NMR and FTIR. Melting temperatures can be controlled over a 60 °C range and glass transition temperature over 40 °C. Melting temperatures are incident with *n*-paraffin molecules having lengths similar to the static methylene sequence length between PEG branches. The observed thermal data are attributed to the crystallization of the polyethylene backbone, resulting in the exclusion of the PEG branches from the crystal, a result confirmed by X-ray diffraction.

Introduction

Amphiphilic copolymers receive considerable attention in the literature due to the vast array of compositions, morphologies, and properties available in these materials.[1−8] Systems featuring hydrophilic segments, often poly(ethylene glycol) (PEG), and lipophilic segments such as polyethylene (PE) are of interest due to their biocompatibility, propensity for phase segregation, and ability to self-assemble into higher ordered structures.[1−12] Block copolymer architectures are by far the most investigated, which is not surprising as advances living polymerization techniques have facilitated the synthesis of numerous systems with well-defined structures.[3,4,6,8,9,13−16] Amphiphilic graft copolymer architectures have received less attention, likely due to the inability to control composition and structure with the same precision available in block copolymer synthesis. This is particularly true for PE-*g*-PEG systems where only a few examples exist, most of which lack structural control in terms of graft incorporation or distribution.[10]

Well-defined microstructures are essential to fully understand the behavior of amphiphilic graft copolymer model systems. Acyclic diene metathesis (ADMET) polycondensation chemistry is an excellent tool to model polymeric systems that lack such structural regularity when synthesized through other means. A number of ethylene-based copolymers have been modeled in this fashion, from simple ethylene-*co*-α-olefin systems made to mimic industrial polyethylene[17] to materials inaccessible through other means such as poly(ethylene-*co*-vinyl ether)[17−19] and so-called "bio-olefins".[20,21]

We previously reported the synthesis of PEG grafted unsaturated polyolefins with controlled placement of PEG grafts.[11] These polymers contained an overwhelming weight percentage of polyether, and the properties reported reflected this. In that study the polyolefin backbone remained unsaturated; this site of unsaturation in the backbone repeat unit serves as a defect well-known to impede the crystallization of PE.[17] Our recent success in controlling the crystallization behavior and morphology of polyethylene through the incorporation of pendant moieties of various size and polarity[18,22−25] inspired us to further investigate fully saturated versions of these PEG grafted polyethylenes. In this study we synthesized a family of polymers with short glycol chains (four oxyethylene repeat units) attached every 9th, 15th, and 21st carbon along a backbone of polyethylene. By precisely controlling the structure, the relative weight percentages of PE and PEG can be varied and the morphological effects of this architecture systematically probed. Our hope is that by incorporating a pendant group that is immiscible with the PE backbone it may be possible to build a layered or channeled morphology that would have utility in advanced applications.

The precise polymer structures have been confirmed by NMR (^{1}H and ^{13}C). Thermal characterization by differential scanning calorimetry (DSC) reveals properties ranging from semicrystalline to fully amorphous. When the PE and PEG content are nearly equal, the polymer contains a high degree of amorphous content as well as crystalline regions that display variable melting behavior based on thermal history. For the case of the highest amount of polyether incorporation, the material is completely amorphous. The lowest amount of polyether incorporation results in a semicrystalline material; the melting temperature is incident with *n*-paraffin molecules of length similar to the static methylene sequence length between PEG branches. X-ray diffraction experiments confirmed that the crystallinity is a result of the PE backbone, which crystallizes excluding the PEG graft, creating crystalline phases of pure polyolefin dispersed in a matrix of amorphous PEG and PE phases.

* Corresponding author. E-mail: wagener@chem.ufl.edu.

10.1021/ma070513r CCC: $37.00
Published on Web 10/31/2007

Experimental Section

Instrumentation. All ^{1}H NMR (300 MHz) and ^{13}C NMR (75 MHz) spectra were recorded on a Varian Associates Mercury 300 spectrometer. Chemical shifts for ^{1}H and ^{13}C NMR were referenced to residual signals from $CDCl_3$ (^{1}H: $\delta = 7.27$ ppm and ^{13}C: $\delta = 77.23$ ppm) with 0.03% v/v TMS as an internal reference. Thin layer chromatography (TLC) was performed on EMD silica gel-coated (250 μm thickness) glass plates. Developed TLC plates were stained with iodine absorbed on silica to produce a visible signature. Reaction conversions and relative purity of crude products were monitored by TLC and ^{1}H NMR. Fourier transform infrared (FT-IR) measurements were conducted on polymer films cast from chloroform onto KBr plates using a Bruker Vector 22 infrared spectrophotometer. High-resolution mass spectrometry analyses were performed on a Bruker APEX II 4.7 T Fourier transform ion cyclone resonance mass spectrometer (Bruker Daltonics, Billerica, MA) using electrospray ionization (ESI). The XRD measurements were taken using a Philips X'Pert MRD system using grazing incidence (omega = 3°). Elemental analysis was carried out at Atlantic Microlab Inc. (Norcross, GA).

Molecular weights and molecular weight distributions (M_n/M_w) were determined by gel permeation chromatography (GPC) using a Waters Associates GPCV2000 liquid chromatography system with an internal differential refractive index detector (DRI) and two Waters Styragel HR-5E columns (10 μm PD, 7.8 mm i.d., 300 mm length) at 40 °C. HPLC grade tetrahydrofuran was used as the mobile phase (flow rate = 1.0 mL/min). Retention times were calibrated against polystyrene standards (Polymer Laboratories, Amherst, MA).

Differential scanning calorimetry (DSC) and temperature-modulated differential scanning calorimetry (MDSC) were performed on a TA Instruments Q1000 equipped with a liquid nitrogen cooling accessory calibrated using sapphire and high-purity indium metal. All samples were prepared in hermetically sealed pans (4−7 mg/sample) and were referenced to an empty pan. A scan rate of 10 °C/min was used unless otherwise specified. Modulated experiments were scanned with a 3 °C/min linear heating rate with a modulation amplitude of 0.4 °C and period of 80 s. Melting temperatures are taken as the peak of the melting transition and glass transition temperatures as the midpoint of a step change in heat capacity. Annealing experiments were conducted as follows: samples were heated through the melt to erase thermal history, followed by cooling at 10 °C/min to −150 °C, heated at 10 °C/min to the annealing temperature, held isothermally for 1 h, cooled rapidly to −150 °C, and heated through the melt at 10 °C/min. Data reported reflects this final heating scan.

Materials. All reagents were purchased from Aldrich and used without further purification unless otherwise specified. Grubbs' first-generation catalyst was a gift from Materia, Inc. Diene tosylates **1a**−**c** and tetra(ethylene glycol) monotrityl ether were synthesized according to the literature.[8,12,26,27]

General Procedure for the Synthesis of Trityl-Protected Tetra(ethylene glycol) Monomers (2a−c). Anhydrous DMF (250 mL) was cannula transferred into an oven-dried, three-neck round-bottom flask equipped with a magnetic stirrer and gas inlet and charged with sodium hydride (1.3 equiv, 60% dispersion in mineral oil). The slurry was cooled to 0 °C, and 1.2 equiv of tetra(ethylene glycol) monotrityl ether in 30 mL of anhydrous DMF was added via syringe. Hydrogen evolution was monitored by a bubbler; when gas evoulution ceased, 1 equiv of **1** in 30 mL of anhydrous DMF was added via syringe. The reaction was stirred for 17 h at 0 °C and quenched by pouring into 600 mL of water. The resulting mixture was extracted with diethyl ether, and the combined organics were washed with brine. Concentration afforded a yellow oil which was further purified by column chromatography.

2-(4-Pentenyl)-6-heptenyl-1-tetra(ethylene glycol) Monotrityl Ether (2a). 55% diethyl ether and 45% hexane eluent yielded 3.2 g (55% yield) of colorless oil. ^{1}H NMR (CDCl3): δ (ppm) 1.21−1.52 (br, 9H), 1.98 (q, 4H), 3.21 (t, 2H), 3.29 (d, 2H), 3.50−3.75 (br, 14H) 4.98 (m, 4H), 5.82 (m, 2H), 7.19 (m, 9H), 7.43 (d, 6H). ^{13}C NMR ($CDCl_3$): δ (ppm) 26.09, 30.83, 34.09, 37.86, 63.19, 70.15, 70.35, 70.44, 70.51, 70.56, 74.53, 86.28, 113.92, 126.68, 127.51, 128.48, 138.97, 143.91. ESI/HRMS: $[M + NH_4]^+$ calcd for $NH_4C_{39}H_{52}O_5$, 618.4153; found 618.4128. Anal. (CH) calcd for $C_{39}H_{52}O_5$: C, 77.96; H, 8.72. Found C, 77.91; H, 8.82.

2-(7-Octenyl)-9-decenyl-1-tetra(ethylene glycol) Monotrityl Ether (2b). 25% ethyl acetate and 75% hexane eluent yielded 4.0 g (60% yield) of colorless oil. ^{1}H NMR ($CDCl_3$): δ (ppm) 1.21−1.52 (br, 21H), 1.98 (q, 4H), 3.21 (t, 2H), 3.29 (d, 2H), 3.50−3.75 (br, 14H) 4.98 (m, 4H), 5.82 (m, 2H), 7.19 (m, 9H), 7.43 (d, 6H). ^{13}C NMR ($CDCl_3$): δ (ppm) 26.52, 28.71, 28.92, 29.70, 31.08, 33.58, 37.86, 63.09, 70.13, 70.36, 70.43, 70.50, 70.57, 74.54, 86.29, 113.90, 126.67, 127.52, 128.49, 138.98, 143.92. ESI/HRMS: $[M]^+$ calcd for $C_{45}H_{64}O_5$, 684.48; found 684.4753. Anal. (CH) calcd for $C_{45}H_{64}O_5$: C, 78.90; H, 9.42. Found C, 78.96; H, 9.48.

2-(10-Undecenyl)-12-tridecenyl-1-tetra(ethylene glycol) Monotrityl Ether (2c). 15% ethyl acetate and 85% hexane eluent afforded 1.01 g (34% yield) of colorless oil. ^{1}H NMR (CDCl3): δ (ppm) 1.21−1.52 (br, 33H), 1.98 (q, 4H), 3.21 (t, 2H), 3.29 (d, 2H), 3.50−3.75 (br, 14H) 4.98 (m, 4H), 5.82 (m, 2H), 7.19 (m, 9H), 7.43 (d, 6H). ^{13}C NMR ($CDCl_3$): δ (ppm) 27.03, 29.14, 29.35, 29.71, 29.82, 29.85, 30.28 31.52, 34.01, 38.29, 63.51, 70.57, 70.78, 70.86, 70.92, 70.99, 74.98, 86.71, 114.28, 127.08, 127.92, 128.90, 139.41, 144.32 ESI/HRMS: $[M + NH_4]^+$ calcd for $NH_4C_{51}H_{76}O_5$, 786.6031; found 786.6037. Anal. (CH) calcd for $C_{51}H_{76}O_5$: C, 79.64; H, 9.96. Found C, 79.46; H, 10.03.

General Procedure for ADMET Polymerizations. Monomers were dried under vacuum at 80 °C for 48 h prior to polymerization and transferred to a 50 mL round-bottom flask equipped with a magnetic stir bar. Grubbs first-generation catalyst (300:1 monomer catalyst ratio) was added, and the flask was placed under vacuum at 45 °C for 4 days. Polymerizations were quenched with ethyl vinyl ether (5 drops in degassed toluene), precipitated into acidic methanol to remove catalyst residue, and isolated as an adhesive gum.

Polymerization of 2-(4-Pentenyl)-6-heptenyl-1-tetra(ethylene glycol) Monotrityl Ether. ^{1}H NMR (CDCl3): δ (ppm) 1.21−1.52 (br, 9H), 1.98 (q, 4H), 3.21 (t, 2H), 3.29 (d, 2H), 3.50−3.75 (br, 14H), 5.35 (br, 2H), 7.19−7.36 (m, 9H), 7.43 (d, 6H). ^{13}C NMR ($CDCl_3$): δ (ppm) 26.09, 30.83, 34.09, 37.86, 63.86, 70.72, 71.01, 71.13, 71.27, 71.33, 75.15, 86.67, 127.14, 128.15, 129.15, 130.06 (cis olefin), 130.79 (trans olefin), 144.68. IR (ν, cm^{-1}): 2924, 2852, 1488, 1462, 1447, 1106, 1032, 1010, 966, 745, 760, 705. GPC (THF vs polystyrene standards): $M_w = 9100$ g/mol; PDI (M_w/M_n) = 1.89.

Polymerization of 2-(7-Octenyl)-9-decenyl-1-tetra(ethylene glycol) Monotrityl Ether. ^{1}H NMR ($CDCl_3$): δ (ppm) 1.21−1.52 (br, 21H), 1.98 (q, 4H), 3.21 (t, 2H), 3.29 (d, 2H), 3.50−3.75 (br, 14H), 5.35 (br, 2H), 7.19−7.36 (m, 9H), 7.43 (d, 6H). ^{13}C NMR ($CDCl_3$): δ (ppm) 27.40, 27.84, 29.87, 29.95, 30.32, 30.40, 30.58, 31.96, 33.25, 38.71, 63.91, 70.93, 71.16, 71.23, 71.30, 71.37, 75.32, 87.09, 127.48, 128.32, 129.29, 130.15 (cis olefin), 130.90 (trans olefin), 144.71. IR (ν, cm^{-1}): 2923, 2853, 1489, 1463, 1448, 1108, 1033, 1011, 967, 746, 761, 706. GPC data (THF vs polystyrene standards): $M_w = 47\,300$ g/mol; PDI (M_w/M_n) = 1.85.

Polymerization of 2-(10-Undecenyl)-12-tridecenyl-1-tetra-(ethylene glycol) Monotrityl Ether. ^{1}H NMR ($CDCl_3$): δ (ppm) 1.21−1.52 (br, 33H), 1.98 (q, 4H), 3.21 (t, 2H), 3.29 (d, 2H), 3.50−3.75 (br, 14H), 5.35 (br, 2H), 7.19 (m, 9H), 7.43 (d, 6H). ^{13}C NMR ($CDCl_3$): δ (ppm) 27.08, 29.49, 29.80, 29.93, 30.33, 31.62, 32.87, 38.39, 63.56, 70.58, 70.81, 70.88, 70.95, 71.02, 75.08, 86.76, 127.10, 127.95, 128.95, 130.09 (cis olefin), 130.54 (trans olefin), 144.37 IR (ν, cm^{-1}): 2923, 2853, 1489, 1463, 1448, 1108, 1033, 1011, 967, 746, 761, 706. GPC data (THF vs polystyrene standards): $M_w = 49\,900$ g/mol; PDI (M_w/M_n) = 1.71.

General Procedure for Parr Bomb Hydrogenation of Unsaturated Polymers. Unsaturated, trityl-protected polymers were dissolved in toluene and added to a glass-lined Parr bomb. Wilkinson's catalyst was added, and the bomb was charged with 700 psi of H_2. The reaction was stirred for 3 days at room temperature. The resulting polymers were purified by precipitation

Scheme 1. Copolymer Synthesis[a]

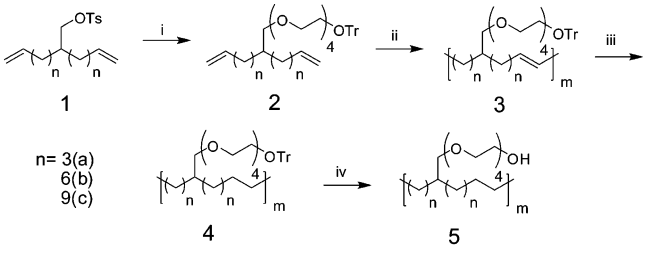

[a] i: NaH, DMF, tetra(ethylene glycol) monotrityl ether; ii: Grubbs' first generation, 45 °C, vacuum; iii: Wilkinson's catalyst, toluene, H_2 700 psi; iv: THF, HCl.

into acidic methanol to remove catalyst residue and isolated as an adhesive gum.

TEGOTr9 (4a). ^{1}H NMR ($CDCl_3$): δ (ppm) 1.21−1.52 (br, 17H), 1.98 3.21 (t, 2H), 3.29 (d, 2H), 3.50−3.75 (br, 14H), 5.35 (br, 2H), 7.19−7.36 (m, 9H), 7.43 (d, 6H). ^{13}C NMR ($CDCl_3$): δ (ppm) 26.19, 30.86, 34.14, 37.82, 63.76, 70.63, 71.05, 71.17, 71.23, 71.41, 75.21, 86.63, 127.16, 128.12, 129.21, 144.68. IR (ν, cm^{-1}): 2924, 2852, 1488, 1462, 1447, 1106, 1032, 1010, 745, 760, 705. GPC (THF vs polystyrene standards): M_w = 9300 g/mol; PDI (M_w/M_n) = 1.63.

TEGOTr15 (4b). ^{1}H NMR ($CDCl_3$): δ (ppm) 1.21−1.52 (br, 29H), 3.29 (t, 2H), 3.21 (d, 2H), 3.50−3.75 (br, 14H), 7.19−7.36 (m, 9H), 7.43 (d, 6H). ^{13}C NMR ($CDCl_3$): δ (ppm) 27.12, 30.03, 30.42, 31.62, 63.55, 70.57, 70.82, 70.90, 70.96, 71.03, 127.13, 127.97, 128.96, 144.38. IR (ν, cm^{-1}): 2923, 2853, 1489, 1463, 1448, 1108, 1033, 1011, 746, 761, 706. GPC (THF vs Polystyrene standards): M_w = 45 100 g/mol; PDI (M_n/M_w) = 1.99.

TEGOTr21 (4c). ^{1}H NMR ($CDCl_3$): δ (ppm) 1.21−1.52 (br, 41H), 3.21 (t, 2H), 3.29 (d, 2H), 3.50−3.75 (br, 14H), 5.35 (br, 2H), 7.19−7.36 (m, 9H), 7.43 (d, 6H). ^{13}C NMR ($CDCl_3$): δ (ppm) 27.08, 29.98, 30.37, 31.62, 38.38, 63.57, 70.58, 70.82, 70.89, 70.96, 71.02, 75.02, 86.76, 127.11, 127.95, 128.95, 144.37 IR (ν, cm^{-1}): 2923, 2853, 1489, 1463, 1448, 1108, 1033, 1011, 967, 746, 761, 720, 706. GPC data (THF vs polystyrene standards): M_w = 51 700 g/mol; PDI (M_w/M_n) = 1.77.

General Procedure for the Removal of the Trityl Protecting Group. The saturated, trityl-protected polymers **4a**−**c** were dissolved in THF, acidified with concentrated HCl, and refluxed for 5 h. The resulting polymers were precipitated into hexane to remove triphenylmethane and dried under vacuum at 80 °C over night to afford an adhesive, elastic gum.

TEGOH9 (5a). ^{1}H NMR ($CDCl_3$): δ (ppm) 1.21−1.52 (br, 17H), 3.29 (d, 2H), 3.50−3.75 (br, 16H). ^{13}C NMR (d_4-methanol): δ (ppm) 26.75, 29.57, 30.53, 31.31, 38.29, 61.08, 70.28, 70.47, 72.56, 74.42. IR (ν, cm^{-1}): 3424, 2924, 2854, 1465, 1351, 1116, 886, 722. GPC (THF vs polystyrene standards): M_w = 9500 g/mol; PDI (M_w/M_n) = 1.57.

TEGOH15 (5b). ^{1}H NMR ($CDCl_3$): δ (ppm) 1.21−1.52 (br, 29H), 3.29 (d, 2H), 3.50−3.75 (br, 16H). ^{13}C NMR (d_8-THF): δ (ppm) 27.93, 30.76, 31.16, 32.52, 39.49, 62.29, 71.50, 71.62, 74.09, 75.03. IR (ν, cm^{-1}): 3423, 2923, 2853, 1464, 1350, 1115, 886, 721. GPC (THF vs Polystyrene standards): M_w = 48 700; PDI (M_n/M_w) = 2.13.

TEGOH21 (5c). ^{1}H NMR ($CDCl_3$): δ (ppm) 1.21−1.52 (br, 41H), 3.29 (d, 2H), 3.50−3.75 (br, 16H), ^{13}C NMR ($CDCl_3$): δ (ppm) 27.34, 29.95, 30.35, 31.55, 38.29, 62.00, 70.60, 70.87, 72.80, 75.04, IR (ν, cm^{-1}): 3422, 2923, 2852, 1463, 1351, 1114, 887, 720. GPC data (THF vs polystyrene standards): M_w = 63 200 g/mol; PDI (M_w/M_n) = 2.19.

Results and Discussion

Synthesis of these precise amphiphilic copolymers involves well-known chemistry (Scheme 1). Diene tosylates **1a**−**c** (prepared as previously described[27]) were coupled with the PEG branch via Williamson etherification. Tetra(ethylene glycol) (TEG) was monoprotected with the bulky trityl (Tr) group before the Williamson etherification to avoid side reactions and enhance solubility in organic media. The structures of monomer **2a**−**c** were confirmed by NMR (^{1}H and ^{13}C), HRMS, and elemental analysis. Following polymerization the unsaturated, trityl-protected polymer was fully hydrogenated using Wilkinson's catalyst. The protecting group remained untouched during this reaction and required subsequent acidification for removal. Polymer structures **3a**−**c** and **4a**−**c** were confirmed by NMR (^{1}H and ^{13}C) and FTIR. Molecular weight data (GPC vs polystyrene standards) are summarized in Table 1.

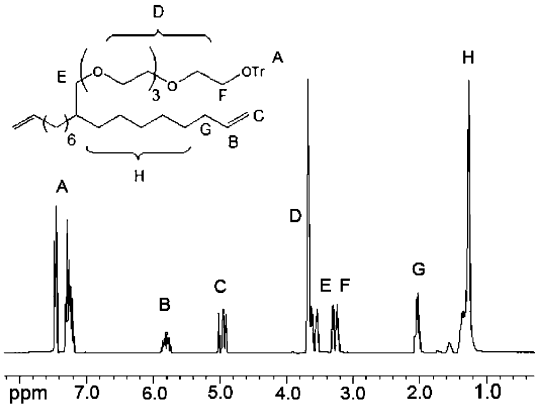

Figure 1. ^{1}H NMR spectrum of **2b**.

Table 1. Molecular Weight Data

polymer	M_n[a] (kg/mol)	M_w[a] (kg/mol)	PDI[b]
TEGOTr9u (**3a**)	4.8	9.1	1.89
TEGOTr15u (**3b**)	25.6	47.3	1.85
TEGOTr21u (**3c**)	29.2	49.9	1.71
TEGOTr9 (**4a**)	5.7	9.3	1.63
TEGOTr15 (**4b**)	22.7	45.1	1.99
TEGOTr21 (**4c**)	29.2	51.7	1.77
TEGOH9 (**5a**)	6.1	9.5	1.57
TEGOH15 (**5b**)	22.9	48.7	2.13
TEGOH21 (**5c**)	28.8	63.2	2.19

[a] GPC vs polystyrene standards. [b] M_w/M_n.

For simplicity of discussion, we adopt a systematic nomenclature for these ADMET amphiphilic copolymers and monomers. Monomers are named first by the number of methylene carbons between the terminal olefin and branch point followed by the identity of the pendant group, for example 66TEGOTr for structure **2b**. Polymers are named first for the identity of the pendant group, followed by the frequency of its appearance along the backbone, e.g., TEGOH15 for structure **5b**. Unsaturated polymers are denoted with the suffix "u". Figure 1 shows the ^{1}H NMR spectrum of 66TEGOTr (**2b,** arbitrarily chosen as an example) with peaks assigned: trityl protecting group (7.2−7.6 ppm), terminal olefin (5.8 and 4.9 ppm), glycol protons (3.5−3.8 ppm), branch point methylene unit (3.3 ppm), methylene unit adjacent to the protecting group oxygen (3.2 ppm), allylic protons (2.1 ppm), and internal methylene protons (1.2−1.6 ppm).

The progression from monomer **2b** to fully saturated, deprotected polymer **5b** by ^{1}H NMR is shown in Figure 2. After polymerization with first-generation Grubbs catalyst the terminal olefin signals at 4.9 and 5.8 ppm in the monomer spectrum converge to one signal for internal olefin at 5.4 ppm in the spectrum of the unsaturated, protected polymer **3**. Following hydrogenation, this internal olefin peak completely disappears in the spectrum of the saturated but still protected polymer **4**. Deprotection with HCl results in the loss of trityl protecting group signal at 7.2−7.6 ppm as seen in the spectrum for the

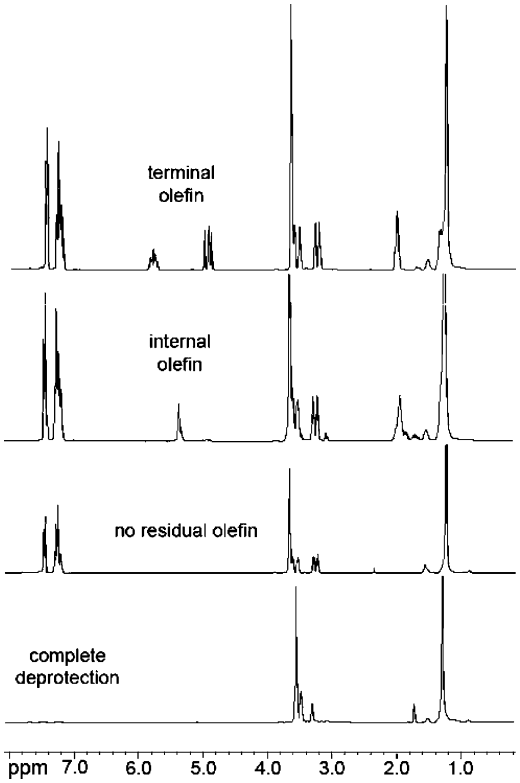

Figure 2. Progression of monomer **2b** to polymer **5b** monitored by ^{1}H NMR.

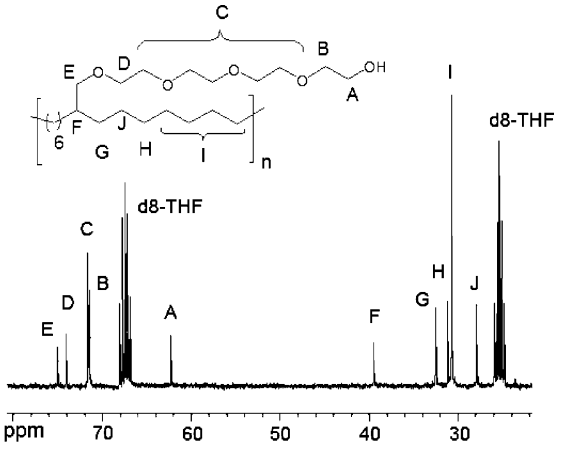

Figure 3. ^{13}C spectrum of TEGOH15 (**5b**).

final polymer **5**. The pristine structures of the fully saturated, deprotected polymers were confirmed by ^{13}C NMR. The spectrum for polymer **5b** is shown in Figure 3; only resonances predicted by the repeat unit are present confirming the absence of side reactions and structural defects.

Thermal Analysis. Figure 4 shows the differential scanning calorimetry (DSC) cycle (first cooling scan from the melt, second heating scan) for the series of saturated, deprotected polymers. TEGOH21 (**5c**) is semicrystalline with a peak melting temperature of 29 °C. Decreasing the space between PEG grafts when moving from TEGOH21 to TEGOH15 (**5b**) results in a decrease in melting temperature from 29 to −3 °C as well as a decrease in melting enthalpy. Both polymers exhibit glass transitions at the same temperature, −63 °C. The marked change in the melting behavior coupled with no change in the thermal response of the amorphous character implies that the crystallinity is solely a result of the PE backbone. This is punctuated by the thermal behavior of TEGOH9 (**5a**), where further decreasing

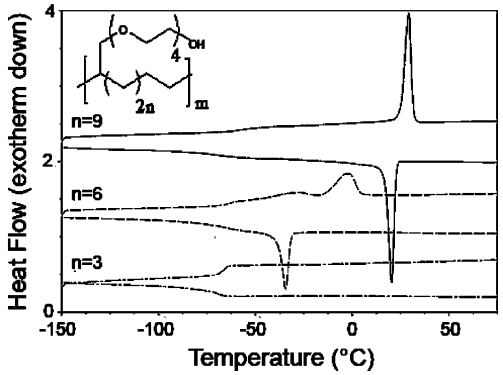

Figure 4. DSC heating and cooling profiles for TEGOH family (**5a**−**c**).

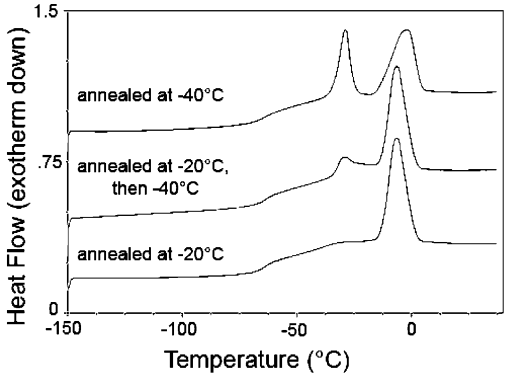

Figure 5. Annealing polymer TEGOH15 (**5b**).

Table 2. DSC Data for Polymers 5a−c

polymer	T_g (°C)	ΔC_p (J/(g °C))	T_m (°C)	ΔH_m (J/g)	T_c (°C)	ΔH_c (J/g)
TEGOH9 (**5a**)	−65	0.73	n/a	n/a	n/a	n/a
TEGOH15 (**5b**)	−63	0.28	−3	19	−34	21
TEGOH21 (**5c**)	−63	0.26	29	36	20	36

the number of backbone carbons between grafts results in a completely amorphous material. The glass transition temperature for TEGOH9, −65 °C, is only slightly depressed from the other polymers in this series, again indicating similar amorphous character. It can be concluded when examining the whole series that for the case of TEGOH21 and TEGOH15 the backbone of the polymer is able to form crystallites while totally excluding the PEG grafts to the amorphous regions. In the case of TEGOH9, the close proximity of the PEG groups along the backbone is disrupting the ability of the backbone to order into crystallites. All three polymers therefore must contain amorphous regions with high polyether content, confirmed by the nearly identical glass transitions. Table 2 summarizes the presented thermal data.

The melting profile of TEGOH15 is particularly interesting as it contains a second, lower temperature endothermic shoulder. Since this material shows only a single, sharp crystallization upon cooling, this shoulder is surprising. Various annealing experiments were conducted to further understand this behavior (Figure 5).

Annealing just below this shoulder induces a significant increase in its intensity without altering the higher temperature endotherm. Annealing just above the shoulder completely suppresses this behavior while slightly affecting the higher temperature endotherm. Annealing first above and then below induces the same effect on the high-temperature peak, but also the reappearance of the lower temperature peak. These annealing treatments should decrease this lower melting transition in all

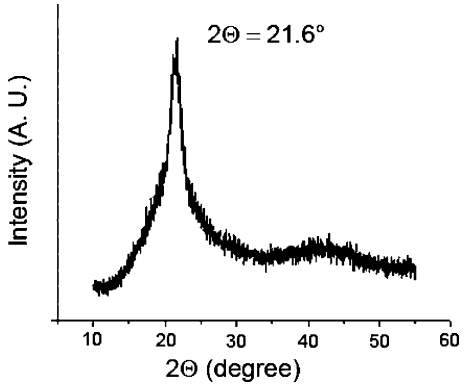

Figure 6. X-ray diffraction pattern for TEGOH21 (**5c**).

cases as the crystallites formed during cooling would provide the template for crystal growth. The low-temperature peak must therefore be an artifact of smaller, less stable crystallites formed after the initial cooling scan.

This behavior was investigated in more depth using temperature-modulated DSC (MDSC). MDSC can provide a wealth of information on overlapping thermal transitions by separating reversible and irreversible processes.[28] On the basis of the MDSC plot (see Supporting Information), crystallization is occurring simultaneously along with melting, beginning just above the glass transition temperature. PE segments that are locked in the amorphous regions upon cooling gain sufficient mobility to crystallize above T_g. As temperature increases, this annealing process continues until finally a maximum melting temperature is reached, and the crystallites formed on cooling melt with no simultaneous crystallization occurring. The low-temperature peak is therefore a result of these smaller crystallites undergoing an annealing process during heating, the higher temperature peak due to the melting of crystallites formed during the cooling scan. Crystallization of the PEG grafts can be ruled out as this phenomenon is not witnessed in the other polymers of this series. Similar behavior is witnessed when annealing experiments are conducted on TEGOH21. When allowed to anneal at room temperature for several days TEGOH21 crystalline perfects, resulting in a peak melting temperature incident with *n*-paraffin molecules with lengths similar to the static methylene sequence length between grafts (see Supporting Information). This result provides more compelling evidence that the crystallinity witnessed in these materials is wholly due to the PE backbone.

Although thermal analysis can provide excellent information on the dynamic crystallization behavior, it provides no information on the structure of the crystallites formed. The thermal data strongly suggest that our PEG graft exclusion model is correct. To be certain, TEGOH21 was studied by X-ray diffraction. TEGOH21 was chosen over TEGOH15 because its melting temperature allows for measurements to be taken at room temperature. The diffraction pattern of TEGOH21 is shown in Figure 6.

A single diffraction is seen at $2\Theta = 21.6°$, which lies in between the known diffraction patterns for orthorhombic paraffins[29] and the $(100)_h$ reflection at $2\Theta = 20.5°$ for hexagonal polyethylene.[30] This implies a contracted hexagonal unit cell tending toward the paraffinic orthorohombic unit cell, almost identical to the results obtained by Wunderlich et al. for poly(octedecyl acrylate),[29] also in agreement with Wegner's[31] assessment of precise alkyl branched polyethylenes prepared by ADMET where the methylene sequences between branches organize into a hexagonal sublattice within a triclinic unit cell. By correlating the XRD and DSC results obtained for these ADMET amphiphiles, it can be concluded that the PE backbone is indeed forming crystallites and excluding the glycol grafts to the amorphous regions.

The terminus of the PEG graft seems to play an extremely important role in this unique behavior. Clustering of the PEG grafts, likely forming a pure polyether phase, is evident by the broad hydrogen-bonding peak in the IR spectrum for these polymers (see Supporting Information). Replacing the hydroxyl end group with the bulky trityl protecting group when going from TEGOH15 to TEGOTr15 disrupts all crystallinity and increases the glass transition temperature by 30 °C (see Supporting Information). The results are similar when moving from TEGOH21 to TEGOTr21; in this case crystallization is not totally disrupted, but it is significantly hindered as noted by a decrease in melting temperature and enthalpy (see Supporting Information). At this point it is unclear whether the lack of hydrogen bonding, the shear steric bulk of the trityl group, or a combination of both is responsible for the difference in behavior between the TEGOH and TEGOTr series.

Conclusions

In summary, amphiphilic PE-*g*-PEG copolymer models with precisely defined structures can be synthesized via metathesis polycondensation chemistry; thermal data suggest that the PE backbones crystallize excluding the PEG graft, a result that is confirmed by X-ray diffraction. Thermal history has a significant effect on behavior of these materials. The identity of the graft end group clearly plays an important role in the morphology of such systems; the copolymer can be made semicrystalline or rendered completely amorphous simply by altering this group. Current synthetic efforts are underway to investigate the effects of different graft end groups and graft lengths to better understand the crystallization behavior and morphology of this class of materials.

Acknowledgment. The authors thank the National Science Foundation (NSF) and the Army Research Office (ARO) for financial support and Materia Inc. for catalyst. The authors also thank Prof. Doug Hirt and Richard Zhou (Clemson University) for interesting and useful discussions. We also thank Dr. Valentin Craciun and Jung Jun Jang of the Major Analytical Instruments Center (MAIC), Department of Materials Science and Engineering at the University of Florida, for assistance with X-ray diffraction and Dr. Cristina Dancel for assistance with HRMS of monomers.

Supporting Information Available: Figures showing modulated DSC of **5b**, annealing **5c**, IR spectra of **5b** and **4b**, and DSC comparison of **4b** and **5b** as well as **4c** and **5c**. This material is available free of charge via the Internet at http://pubs.acs.org.

References and Notes

(1) Liu, G.; Reinhout, M.; Mainguy, B.; Baker, G. L. *Macromolecules* **2006**, *39*, 4726−4734.
(2) Iwasaki, Y.; Akiyoshi, K. *Biomacromolecules* **2006**, *7*, 1433−1438.
(3) Wang, F.; Bronich, T. K.; Kabanov, A. V.; Rauh, R. D.; Roovers, J. *Bioconjugate Chem.* **2005**, *16*, 397−405.
(4) Tian, H. Y.; Deng, C.; Lin, H.; Sun, J.; Deng, M.; Chen, X.; Jing, X. *Biomaterials* **2005**, *26*, 4209−4217.
(5) Cheng, Z.; Zhu, X.; Kang, E. T.; Neoh, K. G. *Langmuir* **2005**, *21*, 7180−7185.
(6) Sun, L.; Liu, Y.; Zhu, L.; Hsiao, B. S.; Avila-Orta, C. A. *Polymer* **2004**, *45*, 8181−8193.
(7) Lu, Y.; Chen, S.; Hu, Y.; Chung, T. C. *Polym. Int.* **2004**, *53*, 1963−1967.
(8) Loiseau, F. A.; Hii, K. K.; Hill, A. M. *J. Org. Chem.* **2004**, *69*, 639−47.

(9) Huang, W.; Zhou, Y.; Yan, D. *J. Polym. Sci., Part A: Polym. Chem.* **2005**, *43*, 2038−2047.
(10) Breitenkamp, K.; Simeone, J.; Jin, E.; Emrick, T. *Macromolecules* **2002**, *35*, 9249−9252.
(11) O'Donnell, P. M.; Brzezinska, K.; Powell, D.; Wagener, K. B. *Macromolecules* **2001**, *34*, 6845−6849.
(12) Chen, Y.; Baker, G. L. *J. Org. Chem.* **1999**, *64*, 6870−6873.
(13) Loiseau, F. A.; Hii, K. K.; Hill, A. M. *J. Org. Chem.* **2004**, *69*, 639−47.
(14) Schmalz, H.; Knoll, A.; Muller, A. J.; Abetz, V. *Macromolecules* **2002**, *35*, 10004−10013.
(15) Guo, Q.; Thomann, R.; Gronski, W.; Thurn-Albrecht, T. *Macromolecules* **2002**, *35*, 3133−3144.
(16) Fukuhara, K.; Hashiwata, K.; Takayama, K.; Matsuura, H. *J. Mol. Struct.* **2000**, *523*, 269−280.
(17) Berda, E. B.; Baughman, T. W.; Wagener, K. B. *J. Polym. Sci., Part A: Polym. Chem.* **2006**, *44*, 4981−4989.
(18) Baughman, T. W.; vanderAa, E.; Wagener, K. B. *Macromolecules* **2006**, *39*, 7015−7021.
(19) Baughman, T. W.; vanderAa, E.; Lehman, S. E.; Wagener, K. B. *Macromolecules* **2005**, *38*, 2550−2551.
(20) Hopkins, T. E.; Wagener, K. B. *Macromolecules* **2004**, *37*, 1180−1189.
(21) Hopkins, T. E.; Pawlow, J. H.; Koren, D. L.; Deters, K. S.; Solivan, S. M.; Davis, J. A.; Gomez, F. J.; Wagener, K. B. *Macromolecules* **2001**, *34*, 7920−7922.
(22) Boz, E.; Nemeth, A. J.; Ghiviriga, I.; Jeon, K.; Alamo, R. G.; Wagener, K. B. *Macromolecules* **2007**, *40*, 6545−6551.
(23) Boz, E.; Nemeth, Alexander, J.; Alamo, Rufina, G.; Wagener, Kenneth, B. *Adv. Synth. Catal.* **2007**, *349*, 137−141.
(24) Baughman, T. W.; Chan, C. D.; Winey, K. I.; Wagener, K. B. *Macromolecules* **2007**, *40*, 6564−6571.
(25) Boz, E.; Wagener, K. B.; Ghosal, A.; Fu, R.; Alamo, R. G. *Macromolecules* **2006**, *39*, 4437−4447.
(26) Sworen, J. C.; Smith, J. A.; Berg, J. M.; Wagener, K. B. *J. Am. Chem. Soc.* **2004**, *126*, 11238−11246.
(27) Smith, J. A.; Brzezinska, K. R.; Valenti, D. J.; Wagener, K. B. *Macromolecules* **2000**, *33*, 3781−3794.
(28) Wunderlich, B. *J. Therm. Anal. Calorim.* **2006**, *85*, 179−187.
(29) Qiu, W.; Sworen, J.; Pyda, M.; Nowak-Pyda, E.; Habenschuss, A.; Wagener, K. B.; Wunderlich, B. *Macromolecules* **2006**, *39*, 204−217.
(30) Uehara, H.; Kanamoto, T.; Kawaguchi, A.; Murakami, S. *Macromolecules* **1996**, *29*, 1540−1547.
(31) Lieser, G.; Wegner, G.; Smith, J. A.; Wagener, K. B. *Colloid Polym. Sci.* **2004**, *282*, 773−781.

MA070513R